INSTITUTE OF PHYSICS PUBLISHING SMART MATERIALS AND STRUCTURES
Smart Mater. Struct. **13** (2004) 873–880 PII: S0964-1726(04)79024-2

Algorithms for active vibration isolation on spacecraft using a Stewart platform

Brij N Agrawal and Hong-Jen Chen

Spacecraft Research and Design Center (SRDC), Department of Mechanical and Astronautical Engineering, Naval Postgraduate School, Monterey, CA 93943, USA

E-mail: agrawal@nps.edu and hchen@nps.edu

Received 26 November 2003, in final form 15 March 2004
Published 16 June 2004
Online at stacks.iop.org/SMS/13/873
doi:10.1088/0964-1726/13/4/025

Abstract
This paper presents the recent development in algorithms for active vibration isolation on spacecraft using a Stewart platform. The multiple error least mean square (LMS) algorithm and the clear box algorithm have been implemented on these platforms and several enhancements have been made to the clear box algorithm. Based on experimental results, it is concluded that the multiple error LMS algorithm is preferred for vibration isolation when a disturbance correlated signal is available. In the absence of such a signal, the clear box algorithm is the method of choice. Among the implementations of the clear box algorithm, the sine/cosine method is preferred for handling time-invariant disturbance frequencies, the adaptive method for rapidly varying disturbance frequencies, and the frequency-domain method for a large number of time invariant disturbance frequencies.

1. Introduction

For an imaging spacecraft, the vibration isolation of its optical payload has been a challenging problem. The problem will become even more challenging on future space missions as the increased performance requirements for the payloads require low vibration and the vibration sources on the spacecraft are increasing due to large flexible structures. Examples of such devices as the vibration sources include cryo-coolers, fluid pumps and other mechanical devices, in addition to reaction wheels and solar array drives. The need to develop improved techniques for vibration isolation has been recognized for more than a decade by several organizations such as NASA and USAF. These organizations initiated several research programs in this area, such as Control Structure Interaction (CSI) by the Jet Propulsion Laboratory (JPL) [1, 2], to develop improved techniques and validate them by ground and in-orbit experiments.

Passive isolation presents a reliable, low cost solution that is effective for attenuating broadband high frequency vibrations. However, it is in general not suited for low frequency vibration isolation since the resulting mechanism is (usually) too soft to withstand the launch environment. Since a spacecraft has low frequency vibrations due to the excitation of flexible structures and the rotating devices, such as solar array drives, cryo-pumps, and reaction wheels, active techniques for low frequency vibration isolation are a desirable approach.

Active vibration isolation allows significant performance enhancements over passive methods, but requires sensors, actuators, and processors, which must be reliable and efficient in mass and power consumption. However, with the development of smart sensors and actuators and the availability of powerful microprocessors, active vibration is becoming an attractive choice for vibration isolation.

Active control techniques for rejection of disturbances are numerous, and include classical feedback, modern feedback, disturbance accommodating control, disturbance observers, repetitive control, adaptive control, adaptive inverse control, adaptive feedforward control, and neural networks [3]. In most cases, narrowband vibrations (periodic disturbances) are most effectively controlled through the use of feedforward techniques.

A widely used adaptive feedforward method for noise and vibration control is the filtered-x LMS algorithm [4] and its multi-input multi-output (MIMO) implementation called the multiple error LMS algorithm [5]. A drawback of these methods is that they require a separately measured disturbance-correlated reference signal, which is adaptively filtered to form

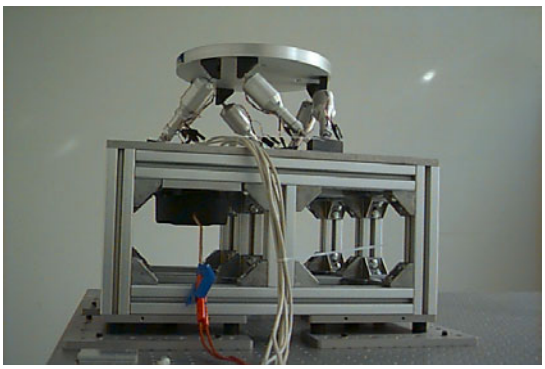

Figure 1. UQP and satellite bus mockup.
(This figure is in colour only in the electronic version)

the control signal. LMS-derived methods also require prior knowledge of the system dynamics, which may vary with time. A new technique that addresses these issues is called the clear box algorithm, and it approaches the control problem from a system identification perspective [6, 7]. Using only knowledge of the actuator inputs and disturbance-corrupted sensor outputs, it allows the identification of both the system dynamics and the disturbance frequencies, and then uses the information to cancel the disturbance. Therefore this technique has the advantage that it does not need a disturbance-correlated signal.

At the Spacecraft Research and Design Center of Naval Postgraduate School, there are three experimental platforms being used in active vibration isolation research, namely, the NPS space truss [8], the positioning hexapod [9], and the ultra quiet platform (UQP). These platforms have one thing in common: they all use smart struts, i.e. struts that are integrated with actuators and sensors into units which, when incorporated with adaptive algorithms, become 'smart' struts capable of performing vibration isolation or positioning without very little user participation.

In this paper, we present the vibration isolation techniques developed and implemented on the Stewart platform UQP. The hardware description of this experimental platform is given in detail in section 2, followed by the explanation of the theory of all implemented control algorithms in section 3. The control algorithms include the multiple error LMS algorithm, the time-domain clear box algorithm, and batch-mode frequency domain clear box algorithm with two enhancements: phase cancellation repetitive control for improving isolation performance between repetitions and quadratic programming for selective disturbance cancellation. The experimental results are then shown in section 4 followed by the conclusions in section 5.

2. Experimental platform

The ultra quiet platform (UQP), as shown in figure 1, is used for testing control algorithms for the vibration isolation of an imaging payload from spacecraft. It is configured similar to a 'cubic' Stewart platform where the struts are arranged as if they were on the edges of a cube, providing three orthogonal pairs of actuators.

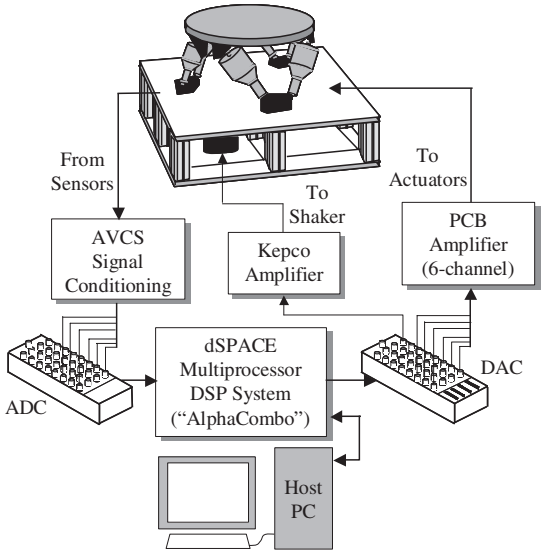

Figure 2. Experiment overview.

In such arrangements, control in six degrees of freedom is possible using linear actuators, and the coupling between actuators is minimized. The UQP is mounted on a spacecraft mockup, to which is mounted the disturbance source. The entire experiment sits on 16 rubber feet attached to a 3800 lb RS4000 Optical Table (Newport Corporation) which uses four I-2000 Series Pneumatic Isolators (Newport Corporation) to help further isolate the experiment from floor vibrations.

Each strut consists of a piezoceramic stack actuator and a geophone sensor. The actuator converts control signal voltages to physical movement of the strut. The maximum displacement of the actuator is 50 μm, which is sufficient for vibration applications, but not for platform pointing or steering. The GS-11D rotating coil geophone sensors (Geo Space) consists of wire coils supported by soft springs under the influence of a magnetic field, which provides a signal proportional to velocity. The source of disturbance for the disturbance rejection experiment, an AST-1B-4 Bass Shaker (Aura Systems), delivers a peak force of 89 N with a resonance frequency of around 40 Hz.

The experimental setup is shown in figure 2 above. The experiment requires power amplification for the actuators and signal conditioning for the geophone sensors. These are provided via a 790A06 Six-Channel Power Amplifier (PCB Piezotronics—peak voltage 200 V, peak current $\pm$50 mA), and a CSA engineering active vibration control system (AVCS) signal-conditioning unit, respectively. The control function is performed by the combination of a DS1003 Alphacombo DSP system (dSPACE) for real time control and a host PC for high level supervisory control. Coding for the control algorithms is performed in the MATLAB/SIMULINK (Mathworks) environment using C-coded 'S-functions' to perform the more specialized tasks.

3. Control algorithms

The current focus of the active vibration isolation for the spacecraft at the SRDC of NPS is the rejection of narrowband periodic disturbances. Adaptive feedforward algorithms, such

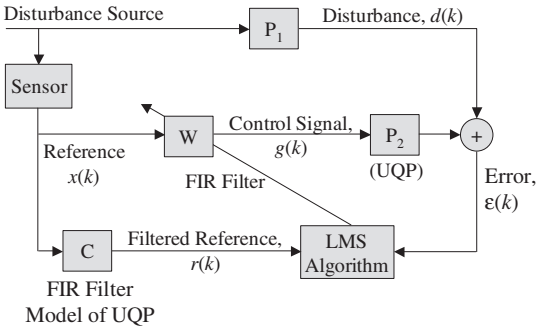

Figure 3. Multiple error least mean square algorithm.

as the widely used multiple error least mean square algorithm and the more recent clear box algorithm, can be used to cancel such disturbances more effectively than the traditional feedback control methods. Both of these algorithms were implemented using MIMO schemes due to the nature of the application on the experimental platforms. In this section the theories of both algorithms are outlined and the foundation of the two enhancements made to the clear box algorithm are laid out.

3.1. Multiple error least mean square algorithm

The least mean square (LMS) algorithm uses an nth order digital finite impulse response (FIR) filter to generate a feedforward control signal $y(k)$ and minimize the mean square error of $\varepsilon(k)$, which represents the difference between $y(k)$ and the disturbance signal $d(k)$. The algorithm requires a reference signal $x(k)$ that is correlated with the disturbance signal $d(k)$ in order for the controller to perform well. The LMS algorithm acts to minimize $\varepsilon(k)$ by directing the filter coefficients towards the minimum point of a quadratic performance surface of $\varepsilon(k)$.

The block diagram of the multiple error LMS algorithm is shown in figure 3. We assume that there are M actuators and L sensors. There is a reference signal $x(k)$ which passes through a primary plant (P_1) before being sensed at the system output as $d(k)$. The disturbance at the lth sensor is represented by $d_l(k)$.

The linear plant model used to filter the reference signal is a Jth order FIR filter, C, whose coefficients c_{lmj} indicate the jth coefficient ($j = 1, \ldots, J$) for the filter that models the dynamics between the mth actuator and the lth sensor. Due to the time-invariant nature of the UQP, a state space multiple-input multiple-output model can be obtained offline in advance using the system identification method OKID [10], then it can be converted to the FIR format. The resulting filtered signal, $r(k)$, includes $L \times M$ elements similarly indicated by $r_{lm}(k)$. The M control signals in $g(k)$ are generated by filtering the reference signal with an Ith order FIR filter W whose coefficients are w_{mi}. Finally, the error signal at each of the L sensors is indicated by $\varepsilon_l(k)$, an expression for which is

$$\varepsilon_l(k) = d_l(k) + \sum_{m=1}^{M} \sum_{j=0}^{J-1} c_{lmj} \sum_{i=0}^{I} w_{mi}(n-j)x(n-i-j). \quad (1)$$

As long as each $d_l(k)$ is partially correlated with $x(k)$ it is possible to reduce the error at each sensor through the proper choice of the coefficients w_{mi}. By defining the total error as

$$T = E\left\{\sum_{l=1}^{L} \varepsilon_l^2(k)\right\}, \quad (2)$$

it is clear that T is a quadratic function of each of the coefficients w_{mi}, indicating that gradient descent methods allow convergence to the global minimum of T. The differentiation of T with respect to one coefficient is

$$\frac{\partial T}{\partial w_{mi}} = 2E\left\{\sum_{l=1}^{L} \varepsilon_l(k) \frac{\partial \varepsilon_l(k)}{\partial w_{mi}}\right\}. \quad (3)$$

Differentiating equation (1) with respect to w_{mi} we obtain

$$\frac{\partial \varepsilon_l(k)}{\partial w_{mi}} = \sum_{j=0}^{J-1} c_{lmj} x(k-i-j). \quad (4)$$

The above signal is the same as that obtained by filtering the reference signal with the FIR filter, C, but delayed by i sample times. Denoting it (this filtered and delayed reference signal) by $r_{lm}(k-i)$, we have

$$\frac{\partial \varepsilon_l(k)}{\partial w_{mi}} = r_{lm}(k-i). \quad (5)$$

Adjusting each filter coefficient in w by the negative of the gradient expression in equation (3), with expected values in (2) and (3) approximated by their instantaneous values, and using the expression in equation (5), we obtain

$$w_{mi}(k+1) = w_{mi}(k) - 2\mu \sum_{l=1}^{L} \varepsilon_l(k) r_{lm}(k-i) \quad (6)$$

where μ is the adaptation rate.

The maximum adaptation rate of μ that can be used without causing instability is given by

$$0 < \mu < \frac{1}{\lambda_{\max}} \quad (7)$$

where $\lambda_{\max}$ is the largest eigenvalue of the correlation matrix of the reference signal x [11]. An alternative upper bound is the inverse value of the trace of the correlation matrix, which is more restrictive but easier to calculate [12].

Note that there is the assumption of time invariance in the w_{mi} filter coefficients and it is equivalent, in practice, to assuming that the filter coefficients change only slowly compared to the timescale of the response of the system to be controlled.

3.2. Time domain clear box algorithm

As mentioned earlier, two drawbacks of the multiple error LMS algorithm are the need of a disturbance correlated signal and the prior knowledge of the system to perform the disturbance rejection. The clear box algorithm addresses both issues with the capability of complete identification of both the system and the unknown periodic disturbance, and then uses the obtained information to form the adaptive feedforward disturbance

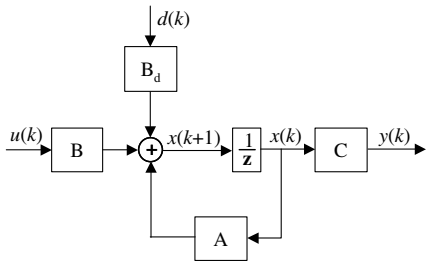

Figure 4. System representation.

cancellation signal. For the development of the clear box algorithm consider the system

$$\begin{aligned} x(k+1) &= Ax(k) + Bu(k) + B_d d(k) \\ y(k) &= Cx(k) \end{aligned} \tag{8}$$

where there are m inputs, q outputs, and n states. Thus $x(k)$ is an $n \times 1$ state vector, $u(k)$ is an $m \times 1$ input vector, and $y(k)$ is a $q \times 1$ output vector. Similarly the system A, B, and C matrices have dimensions $n \times n$, $n \times m$, and $q \times n$, respectively. The system is represented in figure 4. It is assumed that nothing is known except for the recorded system input $u(k)$, the disturbance-corrupted output data measurements $y(k)$, an upper bound on the true system order, n, and an upper bound on the number of frequencies, f, in the disturbance, $d(k)$.

By a process outlined in [3], the control (or excitation) input $u(k)$ and disturbance-corrupted output $y(k)$ satisfy a pth order input–output model,

$$\begin{aligned} y(k) &= \alpha_1 y(k-1) + \alpha_2 y(k-2) + \cdots + \alpha_p y(k-p) \\ &\quad + \beta_1 u(k-1) + \beta_2 u(k-2) + \cdots + \beta_p u(k-p) \end{aligned} \tag{9}$$

as long as p is chosen to be sufficiently large such that

$$p \geqslant \frac{n + 2f + 1}{q} \tag{10}$$

where f is the number of disturbance frequencies in $d(k)$, and the 1 accounts for a non-zero bias in the disturbance (if present). Notice that in this model the disturbance input $d(k)$ does not appear explicitly although it contributes to the data. Its information is completely absorbed in the coefficients α and β, which are referred to here as 'disturbance-corrupted' coefficients.

3.2.1. Disturbance identification through modal decomposition. To facilitate the removal of the disturbance modes it is convenient to convert the ARX (Auto-Regressive with eXogenous input) model to an equivalent state space observable canonical form

$$\begin{aligned} z(k+1) &= A_p z(k) + B_p u(k) \\ y(k) &= C_p z(k) \end{aligned} \tag{11}$$

where

$$A_p = \begin{bmatrix} \alpha_1 & 1 & 0 & \cdots & 0 \\ \alpha_2 & 0 & 1 & \ddots & \vdots \\ \alpha_3 & 0 & 0 & \ddots & 0 \\ \vdots & \vdots & \vdots & \ddots & 1 \\ \alpha_p & 0 & 0 & \cdots & 0 \end{bmatrix}, \qquad B_p = \begin{bmatrix} \beta_1 \\ \beta_2 \\ \beta_3 \\ \vdots \\ \beta_p \end{bmatrix}, \tag{12}$$

$$C_p = [\,1 \quad 0 \quad 0 \quad \cdots \quad 0\,].$$

Conversion of this model to modal form yields the state space equations

$$\begin{aligned} w(k+1) &= \Lambda w(k) + \Gamma u(k) \\ y(k) &= \Omega w(k) \end{aligned} \tag{13}$$

where Λ, Γ, and Ω are formed via similarity transformation:

$$\Lambda = T^{-1} A_p T, \qquad \Gamma = T^{-1} B_p, \qquad \Omega = C_p T. \tag{14}$$

Typically, if p is chosen large enough, the damping ratios of the disturbance modes will be at least one or two orders of magnitude smaller than those of the noise modes or true system modes, and thus (the disturbance modes) can be easily identified. Also, the accuracy of the identified frequency improves as p increases. Once the disturbance modes have been identified in the modal state space model, they can be selectively removed by eliminating the corresponding rows and columns from Λ, Γ, and Ω. The 'disturbance-free' model is then converted to an equivalent ARX model with coefficients $[\bar{\alpha}_1, \bar{\alpha}_2, \ldots, \bar{\alpha}_p]$ and $[\bar{\beta}_1, \bar{\beta}_2, \ldots, \bar{\beta}_p]$. Thus the disturbance-corrupted output can be expressed as

$$\begin{aligned} y(k) &= \bar{\alpha}_1 y(k-1) + \bar{\alpha}_2 y(k-2) + \cdots + \bar{\alpha}_p y(k-p) \\ &\quad + \bar{\beta}_1 u(k-1) + \bar{\beta}_2 u(k-2) + \cdots + \bar{\beta}_p u(k-p) + \eta(k) \end{aligned} \tag{15}$$

where the right-hand side of equation (15) is driven by disturbance corrupted outputs. The disturbance effect, $\eta(k)$, can be calculated in real time by rearranging equation (15) as

$$\begin{aligned} \eta(k) &= y(k) - \bar{\alpha}_1 y(k-1) - \bar{\alpha}_2 y(k-2) - \cdots - \bar{\alpha}_p y(k-p) \\ &\quad - \bar{\beta}_1 u(k-1) - \bar{\beta}_2 u(k-2) - \cdots - \bar{\beta}_p u(k-p). \end{aligned} \tag{16}$$

At this point the disturbance-free system model and the disturbance effect are known, and from equation (16), setting all output $y(k)$ to zero, the feedforward control $u_{\mathrm{f}}(k)$, that cancels steady-state disturbances, satisfies

$$\bar{\beta}_1 u_{\mathrm{f}}(k-1) + \bar{\beta}_2 u_{\mathrm{f}}(k-2) + \cdots + \bar{\beta}_p u_{\mathrm{f}}(k-p) = -\eta(k). \tag{17}$$

3.2.2. Sine/cosine method. The clear box algorithm takes advantage of the knowledge that the control signal, $u_{\mathrm{f}}(k)$, needs to be made up of periodic components in order to cancel periodic disturbances. The first option for generating such a $u_{\mathrm{f}}(k)$, as employed in [6], is to use a sine/cosine pair for each disturbance frequency. For L identified disturbances, the assumed form of the control signal

$$u_{\mathrm{f}}(k) = \sum_{i=1}^{L} [a_i \cos(\omega_i k \Delta t) + b_i \sin(\omega_i k \Delta t)] \tag{18}$$

is substituted into equation (17) and the resulting set of equations (linear in the coefficients a_i and b_i) is solved in real time using recursive least squares (RLS), and employing a 'forgetting factor' λ_{f} to weight recent data more heavily. The control signal in equation (18) is thus a combination of sine and cosine functions, whose L frequencies are estimated using methods outlined in the previous section.

3.2.3. Adaptive basis method. An alternative [13, 14] to using the sine and cosine functions as the bases for synthesizing the disturbance rejection signal, $u_f(k)$, for the clear box algorithm, is to use the N-sample shifted versions of the disturbance effect signal, $\eta(k)$.

For this 'adaptive basis method', the control signal is formed from $\eta(k)$ as follows:

$$u_f(k) = \psi_1\eta(k-\Delta_1) + \psi_2\eta(k-\Delta_2) + \cdots + \psi_N\eta(k-\Delta_N) \tag{19}$$

where $N \geqslant 2f+1$. The Δ_i values ($i = 1, \ldots, N$) are the number of samples that the disturbance effect would need to shift to generate each of the N basis functions that are then linearly combined to form the control signal. Each Δ_i value is preselected by the operator, and the guidelines below should be followed.

$$\begin{aligned} \Delta_i &\geqslant 1 \qquad \text{for all } i \\ \Delta_i &\neq \Delta_j \qquad \text{for all } i, j \\ |\Delta_i - \Delta_j| &\neq |\Delta_j - \Delta_k| \qquad \text{for all } i, j, k. \end{aligned} \tag{20}$$

The first guideline prevents any problems with causality by using the disturbance effect that is delayed by at least one time sample. The second ensures that two functions do not have the same time shift (such a pair would be identical functions). The third introduces a random characteristic to the time shifting, and prevents linear dependence of the basis functions for any given disturbance frequency. The control coefficients in equation (19), ψ_i, where $i = 1, \ldots, N$, are recursively estimated in the same manner as with the sine/cosine method.

There are two basic advantages associated with the adaptive basis approach. First, it eliminates the need to estimate the disturbance frequencies. Second, since the disturbance effect signal $\eta(k)$ is calculated in real time, it contains the exact frequency content of the actual disturbances. Any change in the disturbance frequencies immediately appears in the disturbance effect signal, making the adaptive basis approach capable of handling time-varying disturbance frequencies.

3.3. Frequency domain clear box algorithm

The frequency domain clear box algorithm [15] parallels the development of its time domain counterpart. It is the analog equivalent with two enhancements. First, a phase cancellation repetitive control algorithm [16] is added to the process of generating a feedforward cancellation signal. Zero tracking error, i.e. output error suppressed down to practically the background noise level, is produced through the integration action along with repetitions. Second, when the situation of limited control authority is encountered, the yes-or-no decision algorithm on deciding which disturbance frequencies to control is replaced by a quadratic programming algorithm, which allows partial control of certain disturbance frequencies. Therefore actuator saturation is avoided and the overall performance is improved. Computational efficiency is ensured by the application of the FFT for this algorithm, but there are added difficulties in dealing with the noisy data, the leakage effect, and the synchronization issue of online system identification in the presence of periodic disturbances. The following two sections summarize the theoretical background of the enhancements that were made.

3.3.1. Phase cancellation repetitive control. Consider the input–output relationship for the following general time invariant MIMO system:

$$\begin{aligned} x(k+1) &= Ax(k) + Bu(k) + w(k) \\ y(k) &= Cx(k) \end{aligned} \tag{21}$$

where x is the state vector, u is the batch mode repetitive control input vector adding to feedback control command to correct for repeating errors, y is the output vector, and w includes repetitive disturbances as well as the initial command to the feedback controller, which are both of the same period, p. The system is assumed asymptotically stable and the magnitudes of all eigenvalues of A are less than one.

Taking the z-transform of equation (21) and combining terms, we obtain

$$Y(z) = G_c(z)U(z) + R_w(z) \tag{22}$$

where

$$\begin{aligned} G_c(z) &= C(zI - A)^{-1}B \\ R_w(z) &= C(zI - A)^{-1}W(z) \end{aligned} \tag{23}$$

with I being the identity matrix with matching dimensions and $U(z)$ and $W(z)$ being the z-transforms of $u(k)$ and $w(k)$, respectively.

The z-transform version of the repetitive control law is

$$U_j(z) = U_{j-1}(z) + L(z)E_{j-1}(z) \tag{24}$$

where

$$E_{j-1}(z) = Y_d(z) - Y_{j-1}(z) \tag{25}$$

with j representing the repetition number (repetition 0 referring to the initial repetition with no modification to the feedback command), and $L(z)$ and $Y_d(z)$ representing the z-transforms of the time-domain learning coefficients and the desired output, respectively.

Applying equations (22) and (24), after manipulations, one obtains

$$Y_j(z) = [I - L(z)G_c(z)]Y_{j-1}(z) + L(z)G_c(z)Y_d(z) \tag{26}$$

and

$$E_j(z) = [I - L(z)G_c(z)]E_{j-1}(z) \tag{27}$$

which relate the output and error profiles from one repetition to the next. Using recursive substitution in equations (26) and (27) gives

$$Y_j(z) = [I - L(z)G_c(z)]^j Y_0(z) + \{I - [I - L(z)G_c(z)]^j\}Y_d(z) \tag{28}$$

and

$$E_j(z) = [I - L(z)G_c(z)]^j E_0(z) \tag{29}$$

where the subscript 0 indicates the initial trial repetition.

It is then recognized that the condition needed for convergence to zero error is

$$|\lambda_i| < 1, \qquad i = 1, 2, \ldots, q \tag{30}$$

where the λ_i are the eigenvalues of $I - L(z)G_c(z)$ and q is the number of outputs. Considering the steady-state frequency response, and setting $z = e^{j\omega T}$ where T is the sample time, the

learning therefore produces monotonic decay of every steady-state discrete frequency components of the error. For the case of a SISO system, equation (30) reduces to

$$|1 - L(e^{j\omega T})G_c(e^{j\omega T})| < 1, \qquad i = 1, 2, \ldots, q. \tag{31}$$

This is a sufficient condition for convergence, and also a condition for good transients during the repetitive control process, producing a monotonic convergence in the steady-state response. Thus it is a performance condition that requires the Nyquist plot of $L(e^{j\omega T})G_c(e^{j\omega T})$ to be within a unit circle centered on the real axis at unit positive distance.

The phase cancellation repetitive control law, for the case of a SISO system, is given as

$$L(e^{j\omega_k T}) = \begin{cases} -\angle G_c(e^{j\omega_k T}), & \text{if } |G_c(e^{j\omega_k T})| \leqslant 1 \\ -\dfrac{\angle G_c(e^{j\omega_k T})}{|G_c(e^{j\omega_k T})|}, & \text{if } |G_c(e^{j\omega_k T})| > 1 \end{cases} \tag{32}$$

where $\omega_k = \frac{2\pi k}{NT}$, $k = 0, 1, \ldots, N-1$ and $G(e^{j\omega_k T})$ is the frequency response of the system at the N discrete frequencies ω_k.

This repetitive control law actually puts all points on the Nyquist plot of $L(e^{j\omega T})G_c(e^{j\omega T})$ on the real axis between the origin and +1. Therefore it satisfies the unit circle performance condition (31) for all N discrete frequencies at ω_k.

For a MIMO system with square and diagonalizable system frequency response function at every frequency, the learning gain matrix is

$$L(e^{j\omega_k T}) = V^{-1}(e^{j\omega_k T})\Lambda_L(e^{j\omega_k T})V(e^{j\omega_k T}) \tag{33}$$

where V and Λ_ϕ are the eigenvector and the eigenvalue matrices of the transfer matrix $G_c(e^{j\omega_k T})$, and the eigenvalues of the matrix Λ_L are

$$\lambda_i(e^{j\omega_k T}) = \begin{cases} -\angle\lambda_i[G_c(e^{j\omega_k T})], & \text{if } |\lambda_i[G_c(e^{j\omega_k T})]| \leqslant 1 \\ -\dfrac{\angle\lambda_i[G_c(e^{j\omega_k T})]}{|\lambda_i[G_c(e^{j\omega_k T})]|}, & \text{if } |\lambda_i[G_c(e^{j\omega_k T})]| > 1 \end{cases} \tag{34}$$

where $\omega_k = \frac{2\pi k}{NT}$, $k = 0, 1, \ldots, N-1$ and $i = 0, 1, \ldots, q$, and $G_c(e^{j\omega T})$ and $\lambda_i[G_c(e^{j\omega_k T})]$ are the frequency response of the system and its eigenvalues at all N discrete frequencies at ω_k.

3.3.2. Intelligent error cancellation by quadratic programming. In time domain clear box algorithms, the control computation gives full information as to how much control effort is required to cancel each frequency component of the error, but only yes or no decisions were made when full cancellation requires use of control actions that exceed the actuator limits. The application of quadratic programming to the worst case scenario of multiple disturbance frequencies allows partial cancellation that prevents actuator saturation and produces overall improvement on the tracking accuracy.

Consider a six-input, six-output system subject to the disturbance of five frequencies with limited control authority $u_{\max}$ for each input actuator. Let d_{ij} represent the amplitude of the disturbance frequency i on output j and c_{ij} be the amplitude of the input signal needed to cancel d_{ij}. The maximum possible amplitude of the disturbance on output j is the sum of d_{ij} over i. It occurs when all five frequency components are at their peak values at the same time.

Also define

$\underline{d}_i$ and $\underline{c}_i$ as column vectors of d_{ij} and c_{ij},
α_i as the fraction of input ($0 \leqslant \alpha_i \leqslant 1$) to cancel the disturbance frequency i for all outputs,
β_i as complement of α_i so that $0 \leqslant \beta_i = 1 - \alpha_i \leqslant 1$,
C, D, and $\underline{\beta}$ as column matrices of c_i, d_i, and β_i,
$\underline{1}_5$ and $\underline{1}_6$ as five- and six-dimensional column vectors with all entries equal to one,
$\underline{0}_6$ as six-dimensional column vectors with all entries equal to zero,
and
$u_{\max}$ as the same saturation limit for all actuators.

Then the maximum disturbances vector, i.e., the worst case when all frequency components are at their peak, is

$$\underline{d} = \underline{d}_1 + \underline{d}_2 + \underline{d}_3 + \underline{d}_4 + \underline{d}_5. \tag{35}$$

The maximum magnitude for each input is

$$\begin{aligned} \underline{c} &= \alpha_1\underline{c}_1 + \alpha_2\underline{c}_2 + \alpha_3\underline{c}_3 + \alpha_4\underline{c}_4 + \alpha_5\underline{c}_5 \\ &= C(\underline{1}_5 - \underline{\beta}) \\ &\leqslant u_{\max}\underline{1}_6 \end{aligned} \tag{36}$$

and the maximum remaining disturbance after this fractional cancellation is

$$\underline{d} = \beta_1\underline{d}_1 + \beta_2\underline{d}_2 + \beta_3\underline{d}_3 + \beta_4\underline{d}_4 + \beta_5\underline{d}_5 = D\underline{\beta}. \tag{37}$$

To optimize the amount of each mode to cancel, quadratic programming is used to minimize the objective function

$$J = \underline{d}^{\mathrm{T}}\underline{d} = \underline{\beta}^{\mathrm{T}}D^{\mathrm{T}}D\underline{\beta} \tag{38}$$

with component-by-component inequality constraints

$$\underline{0}_6 \leqslant \beta_i \leqslant \underline{1}_6, \qquad \forall i, \tag{39}$$

and

$$-C\underline{\beta} \leqslant u_{\max}\underline{1}_6 - C\underline{1}_5. \tag{40}$$

4. Experimental results

The effectiveness of the control algorithms is determined by using them on the experimental platforms described in section 2.

Figure 5 shows the identified modes and their associated damping ratios determined by the clear box method. The disturbance modes are identified by the fact that their damping is below the damping threshold, which is set by the user based on the knowledge of the physical system.

The three time-domain controllers, multiple error LMS method, clear box sine/cosine method, and clear box adaptive basis method, were tested for the vibration isolation of a disturbance frequency at 120 Hz. The experiments demonstrate [14] that all three controllers work effectively, reducing the sensor output to the level of the background noise.

Next, the three controllers were tested for a single time-varying disturbance frequency with the profile shown in figure 6.

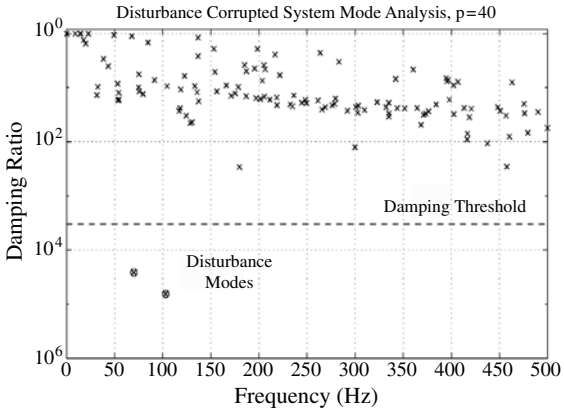

Figure 5. Clear box system identification, analysis of modes.

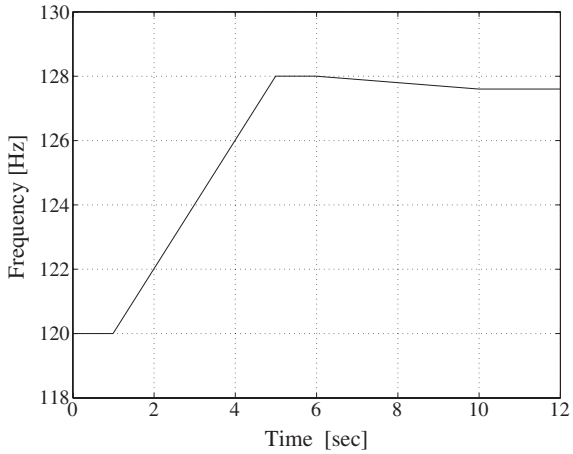

Figure 6. Frequency variation profile, single disturbance.

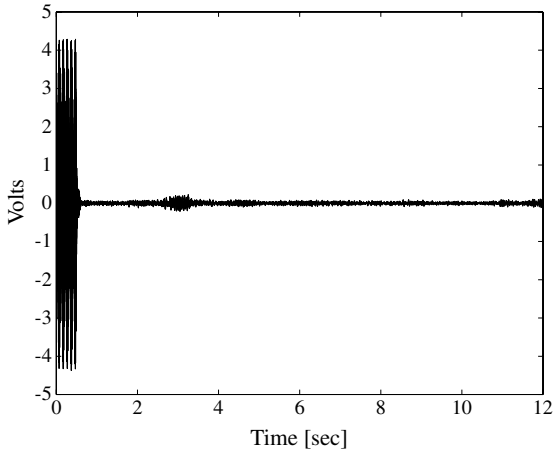

Figure 7. Uncontrolled response and multiple error LMS method response, one varying frequency.

With a good source of well-correlated disturbance signal $x(k)$, the multiple error LMS algorithm performs quite well over the course of the frequency variation profile, as shown in figure 7. Note that figures 7–10 show the output voltage of the geophone sensors, which measure the velocity of the vibration with an intrinsic voltage sensitivity of 0.32 V cm^{-1} s^{-1}.

The performance of the clear box sine/cosine method is shown in figure 8. This method had significant degradation

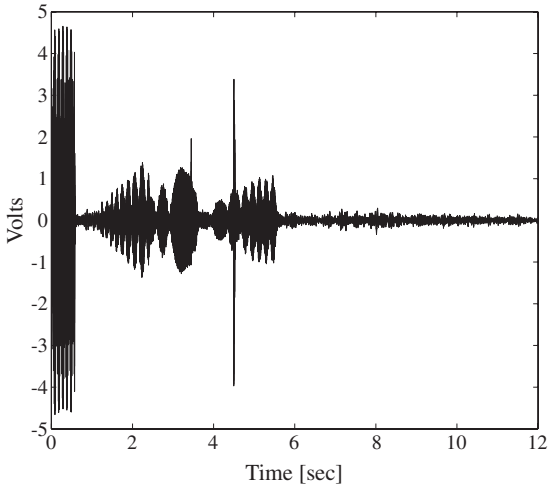

Figure 8. Uncontrolled response and clear box sine/cosine method response, one varying frequency.

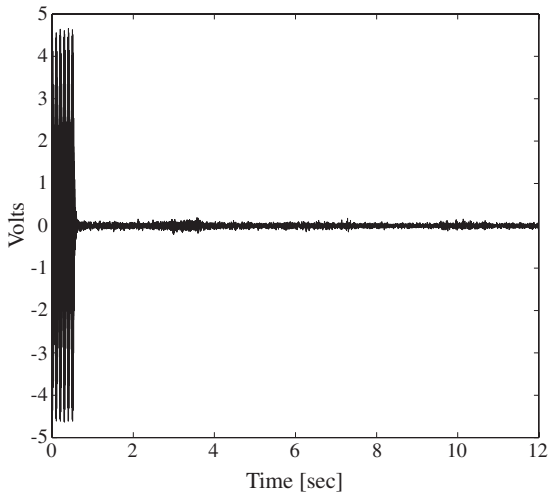

Figure 9. Uncontrolled response and clear box adaptive basis method response, one varying frequency.

in performance during rapid ramp-up in frequency since the frequency estimates (when updated through batch processing once per second) quickly become inaccurate.

The performance of the clear box adaptive method is shown in figure 9. This method is able to maintain good performance, reducing the sensor output to the background noise level. Therefore, this method is effective even if the frequency of the disturbance is varying.

Similar test cases were also run for the frequency domain clear box algorithm implemented in batch mode. Comparable good final level was achieved for the case of time-invariant, single or multiple disturbance frequencies. The algorithm is less computationally intensive than its time domain counterparts. As shown in figure 10, it cancels just as well a disturbance with five frequency components, which is already beyond the computational capacity of our control hardware for the time-domain clear box method. For application to the vibration isolation on spacecraft, such a computational advantage is very important as the computing resources on spacecraft are very limited. But as in the case of the time-domain clear box sine/cosine method, it was unable

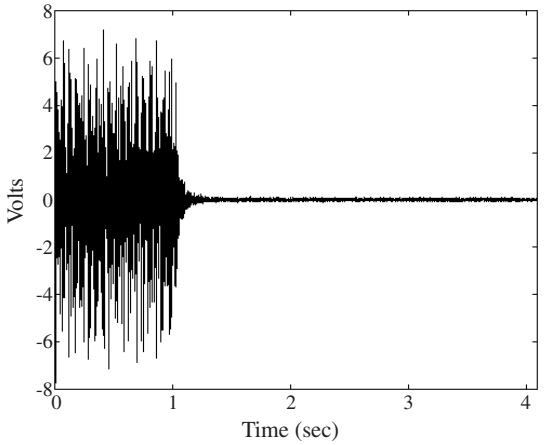

Figure 10. Uncontrolled response and MIMO controlled response of five disturbance frequencies (repetition 10).

to adapt quickly to a variable frequency profile since it was batch-implemented.

5. Conclusions

Based on these experimental results of testing all the algorithms described in this paper on the UQP, we make the following conclusions. The drawbacks of the multiple error LMS algorithm are that tuning of the adaptation rate is necessary to achieve optimal convergence and that it requires disturbance correlated signals. When disturbance-correlated signals are available, it is the preferred control algorithm due to its better computational efficiency. The performance of the clear box method, implemented in either time-domain or frequency domain, meets or exceeds that of the multiple error LMS algorithm without requiring a measured disturbance-correlated signal. When there are no disturbance-correlated signals available, as is the case with the majority of systems, the clear box method is the method of choice. The time domain clear box sine/cosine method is preferred when the disturbance frequencies are time-independent or just varying slowly, but for rapidly varying disturbance frequencies the adaptive basis version should be used. Both of the time domain clear box versions have, however, the drawback of requiring significantly higher processing speed. The frequency-domain clear box method has the drawback of its accuracy issue regarding noisy data sets or the DFT/FFT leakage effect—potentially longer data sets need to be taken per batch and a frequency/amplitude/phase estimate subroutine is required when encountering the situation of non-synchronized sampling rate with disturbance frequencies. It is the preferred approach to handling a large number of time-invariant disturbance frequencies.

Acknowledgments

The authors want to acknowledge the significant contributions made by Lieutenant Colonel Stephan G Edwards, USAF, Professor Richard W Longman of Columbia University, and Professor Minh Q Phan of Dartmouth College on their research work on vibration isolation at the center as reported in this paper.

References

[1] Neat G W, Laskin R A, Regner J W and Van Flotow A 1994 Advanced isolation/precision pointing platform testbed for future spacecraft missions *Advances in the Astronautical Sciences* vol 86 (San Diego, CA: Univelt) pp 37–54

[2] Rahman Z, Spanos J and Laskin R 1997 A six axis vibration isolation, suppression, and steering system for space applications *35th Aerospace Sciences Mtg and Exhibit (Reno, NV, Jan. 1997)*

[3] Goodzeit N E 1998 System and disturbance identification for adaptive disturbance-rejection control *PhD Dissertation* Princeton University, Princeton, NJ

[4] Widrow B and Stearns S D 1985 *Adaptive Signal Processing* (Englewood Cliffs, NJ: Prentice-Hall) pp 288–94

[5] Elliott S J, Stothers I M and Nelson P A 1987 A multiple error LMS algorithm and its application to the active control of sound and vibration *IEEE Trans. Acoust. Speech Signal Process.* **35** 1423–34

[6] Goodzeit N E and Phan M Q 1997 Exact system identification in the presence of completely unknown periodic disturbances *Department of Mechanical and Aerospace Engineering Technical Report No.* 2096 Princeton University, Princeton, NJ
Also, Goodzeit N E and Phan M Q 1997 *J. Guid. Control Dyn.* **23** 251–9

[7] Goodzeit N E and Phan M Q 2000 A clear-box adaptive system for flexible spacecraft identification and disturbance rejection *J. Vib. Control* **6** 757–80

[8] Song G, Vlattas J, Johnson S and Agrawal B N 1999 Active vibration control of a space truss using PZT stack actuator *ASME Int. Mechanical Engineering Congr. & Exposition (Nashville, TN, 1999)* ASME Aerospace Division, vol AD-59 pp 263–8

[9] Chen H J, Bishop R and Agrawal B N 2003 Payload pointing and active vibration isolation using hexapod platforms *11th AIAA/ASME/AHS/ACS Structures, Structural Dynamics and Materials Conf.* vol 3 (Reston, VA: AIAA) pp 2196–214

[10] Minh Q P 1997 *OKID Observer/Kalman Filter Identification: Step-by-Step Guide and Reference* (Princeton, NJ: Department of Mechanical and Aerospace Engineering)

[11] Widrow B and Stearns S D 1985 *Adaptive Signal Processing* (Englewood Cliffs, NJ: Prentice-Hall) p 59

[12] Widrow B and Stearns S D 1985 *Adaptive Signal Processing* (Englewood Cliffs, NJ: Prentice-Hall) p 103

[13] Edwards S G, Agrawal B N, Phan M Q and Longman R W 2000 Disturbance identification and rejection experiments on an ultra quiet platform *Adv. Astronaut. Sci.* **103** 633–51

[14] Edwards S G 1999 Active narrowband disturbance rejection on an ultra quiet platform *PhD Dissertation* Naval Postgraduate School, Monterey, CA

[15] Chen H J, Longman R W, Agrawal B N and Phan M Q 2000 Frequency-domain clear box disturbance rejection *Proc. 10th AAS/AIAA Space Flight Mechanics Mtg (Clearwater, FL, Jan. 2000)*; *Adv. Astronaut. Sci.* **105 I** 73–85

[16] Elci E, Longman R W, Phan M Q, Juang J-N and Ugoletti R 1994 Automated learning control through model updating for precision motion control *Adaptive Structures and Composite Materials: Analysis and Applications* (New York: ASME) pp 299–314 (AD-45/MD-54)